

Fourier Transform Emission Spectroscopy of TaO

R. S. Ram and P. F. Bernath¹

Department of Chemistry, University of Arizona, Tucson, Arizona 85721

Received February 19, 1998; in revised form April 30, 1998

The emission spectrum of TaO, excited in a tantalum hollow cathode lamp, has been observed at high resolution using a Fourier transform spectrometer. In addition to previously known transitions, a number of new bands have been identified and assigned as belonging to two new electronic transitions: $H^2\Pi_{1/2}-X^2\Delta_{3/2}$ and $K^2\Phi_{5/2}-X^2\Delta_{3/2}$. A rotational analysis of the 0–0 and 0–1 bands of the $H^2\Pi_{1/2}-X^2\Delta_{3/2}$ transition and of the 0–1, 1–2, 0–0, 1–0, and 2–1 bands of the $K^2\Phi_{5/2}-X^2\Delta_{3/2}$ transition has been carried out, providing the following equilibrium constants for the ground $X^2\Delta_{3/2}$ state: $\omega_e = 1028.9060(15) \text{ cm}^{-1}$, $\omega_e x_e = 3.58928(66) \text{ cm}^{-1}$, $B_e = 0.40289737(139) \text{ cm}^{-1}$, $\alpha_e = 0.00185445(83) \text{ cm}^{-1}$, and $r_e = 1.6873430(29) \text{ \AA}$. The principal molecular constants for the $H^2\Pi_{1/2}$ state are $T_{00} = 20\,634.32758(40) \text{ cm}^{-1}$, $B_0 = 0.3766867(31) \text{ cm}^{-1}$, and $r_0 = 1.7450604(72) \text{ \AA}$, while the equilibrium constants for the $K^2\Phi_{5/2}$ state are $\omega_e = 905.4549(15) \text{ cm}^{-1}$, $\omega_e x_e = 3.67601(64) \text{ cm}^{-1}$, $B_e = 0.37965102(36) \text{ cm}^{-1}$, $\alpha_e = 0.00189370(21) \text{ cm}^{-1}$, and $r_e = 1.7382343(8) \text{ \AA}$. Although the $H^2\Pi_{1/2}$ and $K^2\Phi_{5/2}$ states have been observed previously in matrix isolation experiments, our work on these states is the first in the gas phase. © 1998 Academic Press

INTRODUCTION

The early transition metal monoxides are species of astro-physical and chemical importance (1, 2). Because of their large dissociation energies and relatively high cosmic abundances, several transition metal diatomic oxides have been found in the atmospheres of cool stars. For example, TiO (3, 4) and YO (5–8) have been identified in the atmospheres of cool *M*-type stars, and ZrO (8) has been identified in *S* stars. TaO has also been tentatively identified in the atmosphere of the *S* star ‘‘R Cyg’’ (8). Transition metal oxides are also important for understanding of chemical bonding in simple metal systems and in heterogeneous catalytic processes involving transition metal elements.

Among the VB family of transition elements the electronic spectra of all monoxides have now been observed. From the gas phase studies of these molecules the ground electronic states of VO (9–11) and NbO (12, 13) have been established as $^4\Sigma^-$ states, while the ground state of TaO (14) has been found to be of $^2\Delta$ symmetry. A number of low-lying electronic states of these molecules have also been characterized from high-resolution studies.

The spectra of TaO have been known for several decades and are relatively well understood. A number of TaO bands were observed in the visible and near ultraviolet regions using arc source excitation (15, 16), and a rotational analysis of some of these bands was initially reported by Premswarup (16) and later on by Premswarup and Barrow (17). The analysis of Premswarup (16) was found to be in error and a revised

analysis by Premswarup and Barrow (17) suggested a $^2\Delta$ ground state for TaO, although they were unable to state definitely whether the ground state was regular or inverted. These studies were followed by a matrix absorption study of TaO and TaO₂ by Weltner and McLeod (18). In this work the molecules were trapped in neon and argon matrices at 4 and 20 K after vaporizing tantalum oxide at 2270 K, and the absorption spectra were observed from the near infrared to the near ultraviolet. The different excited states were labeled using letters ranging from A to Q. All of these transitions involve the $X^2\Delta_{3/2}$ as the lower state consistent with a $^2\Delta_r$ ground state. They also suggested some revision in the rotational analysis of Premswarup and Barrow (17). The spectrum of TaO was then reinvestigated by Cheetham and Barrow (14) using arc as well as radiofrequency excitation in view of the suggestions made by Weltner and McLeod (18). In addition to the bands involving $X^2\Delta_{3/2}$ state, several new transitions were identified as involving the $X^2\Delta_{5/2}$ spin component. The rotational analysis of a large number of TaO bands was obtained and the ground state was confirmed as a $^2\Delta_r$ state with a $^2\Delta_{5/2}-^2\Delta_{3/2}$ separation of 3505 cm^{-1} . Because of large spin–orbit intervals in the different electronic states individual subbands are widely separated, suggesting some Hund’s case (c) behavior. However, the different transitions were labeled using Hund’s case (a) notation (e.g., $^2\Pi_{1/2}$, $^2\Delta_{3/2}$, $^2\Phi_{5/2} \rightarrow ^2\Delta_{3/2}$, and $^2\Pi_{3/2}$, $^2\Delta_{5/2}$, $^2\Phi_{7/2} \rightarrow ^2\Delta_{5/2}$) by Cheetham and Barrow (14).

The magnetic circular dichroism (MCD) spectrum of matrix-isolated TaO was studied by Brittain *et al.* (19), and the total angular momentum quantum number (Ω) for 14 excited states was determined independently. These Ω -assignments were generally consistent with the observations of Cheetham and

¹ Also at Department of Chemistry, University of Waterloo, Waterloo, Ontario, Canada N2L 3G1.

Barrow (14). In addition, the rotational g factors for the ground $X^2\Delta_{3/2}$ and excited $^2\Phi_{5/2}$ states were also determined. The high-temperature photoelectron spectra of TaO and NbO were observed by Dyke *et al.* (20), and their assignments were made with the assistance of *ab initio* calculations. The first adiabatic ionization energies of TaO and NbO were measured as 8.81 ± 0.02 and 7.91 ± 0.02 eV, respectively (20).

A comparison of the matrix absorption spectra (18) with the gas phase spectra of TaO (14) indicates that some of the transitions observed strongly in the matrix spectra were not identified by Cheetham and Barrow (14) in their spectra. In this paper we report on the observation and analysis of two such transitions labeled K and H in the matrix spectra of Weltner and McLeod (18). These transitions have been assigned as $H^2\Pi_{1/2}-X^2\Delta_{3/2}$ and $K^2\Phi_{5/2}-X^2\Delta_{3/2}$ consistent with the Ω -assignments of Brittain *et al.* (19).

EXPERIMENTAL

The emission spectrum of TaO was observed in a tantalum hollow cathode lamp. The cathode was prepared by inserting a 1-mm thick cylindrical foil of tantalum metal into a hole in a copper block. The foil was tightly pressed against the inner wall of the cathode to provide a close and uniform contact between the metal and the copper wall. The initial aim of this experiment was a search for the spectra of TaN by discharging a mixture of neon and a trace of N_2 through the lamp. In addition to a few TaN bands observed previously (21), a number of TaO bands were also observed in the 17000–28000 cm^{-1} region even though O_2 was not added. Probably some oxygen was trapped in the system or some tantalum oxide was present on the surface of the cathode from the reaction of tantalum metal with atmospheric oxygen. The spectrum used in this analysis was recorded with about 2.0 Torr of Ne and 6 mTorr of N_2 at a current of 400 mA at 430 V.

The spectra were recorded using the 1-m Fourier transform

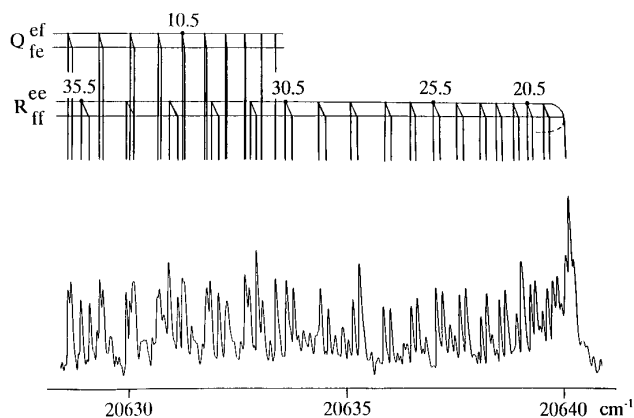


FIG. 1. A portion of the 0–0 band of the $H^2\Pi_{1/2}-X^2\Delta_{3/2}$ transition of TaO near the R head.

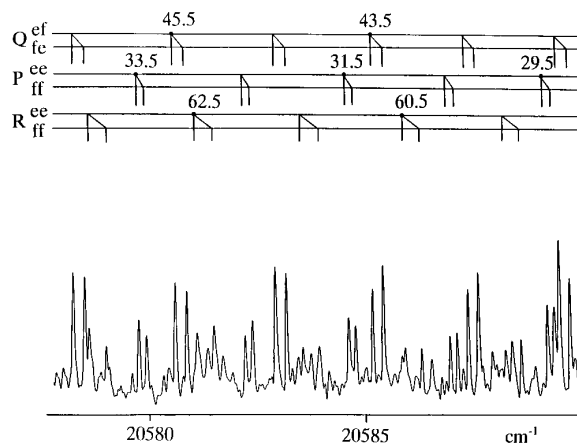


FIG. 2. Some high- J lines of the 0–0 band of the $H^2\Pi_{1/2}-X^2\Delta_{3/2}$ transition of TaO showing Ω -doubling in the P , Q , and R branches.

spectrometer associated with the McMath-Pierce Solar Telescope of the National Solar Observatory. The spectra in the 10 000–20 000 cm^{-1} region were recorded using Si-diode detectors, a quartz beam splitter, and RG495 filters with six scans coadded in 45 min of integration. The spectra in the 19 000–30 000 cm^{-1} interval were recorded with Si-diode detectors and $CuSO_4$ filters and 14 scans were coadded in 80 min of integration. For each setting the spectrometer resolution was 0.02 cm^{-1} .

In addition to the TaN and TaO bands, the final spectra also contained Ta and Ne atomic lines. The Ne atomic lines were used for absolute wavenumber calibration using the measurements of Palmer and Engelman (22). The TaO lines have widths of about 0.06 cm^{-1} and appear with a maximum signal-to-noise ratio of about 15:1, so that the absolute accuracy and precision of measurements of strong and unblended lines is expected to be of the order of ± 0.002 cm^{-1} .

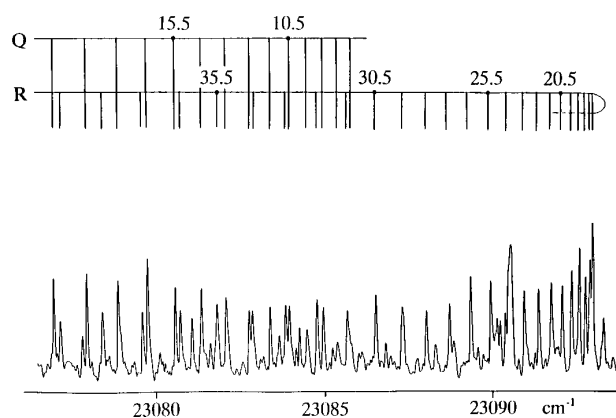


FIG. 3. A portion of the 0–0 band of the $K^2\Phi_{5/2}-X^2\Delta_{3/2}$ transition of TaO near the R head.

TABLE 1
Observed Line Positions (in cm^{-1}) in the $H^2\Pi_{1/2}-X^2\Delta_{3/2}$ Transition of TaO

0 - 0												
J	Ree(J)	O-C	Pee(J)	O-C	Qef(J)	O-C	Qfe(J)	O-C	Rff(J)	O-C	Pff(J)	O-C
6.5					20633.086	9						
7.5					20632.696	2						
8.5					20632.260	-2						
9.5							20631.818	-14				
10.5					20631.241	-5	20631.296	-8				
11.5					20630.651	-10	20630.717	-8				
12.5					20630.019	-7					20620.670	-7
13.5			20619.172	-4	20629.335	-6	20629.409	-7			20619.241	-3
14.5			20617.680	-7	20628.598	-6	20628.675	-9			20617.754	-7
15.5			20616.144	-3			20627.908	5	20640.332	-0	20616.219	-9
16.5			20614.564	7	20626.981	0	20627.069	-2	20640.252	-1		
17.5			20612.915	-2	20626.086	-7						
18.5	20639.835	0	20611.221	-5	20625.151	-4	20625.257	1	20639.945	3	20611.318	-5
19.5	20639.590	-7	20609.476	-9	20624.170	5	20624.269	-3	20639.706	-4	20609.582	-4
20.5	20639.315	5	20607.693	0	20623.117	-9	20623.237	-1	20639.425	-3	20607.802	2
21.5	20638.979	8	20605.854	4	20622.037	2	20622.151	-2	20639.094	-0	20605.957	-7
22.5	20638.577	-5	20603.965	7	20620.891	-2	20621.017	-1	20638.714	3	20604.084	8
23.5	20638.142	1	20602.017	3	20619.703	1	20619.837	5	20638.283	6	20602.136	-2
24.5	20637.649	-1	20600.010	-10	20618.461	1	20618.597	2	20637.798	7	20600.146	-3
25.5	20637.106	-2	20597.981	5	20617.159	-7	20617.302	-5	20637.260	5	20598.108	-2
26.5	20636.521	5	20595.876	-4	20615.828	5	20615.968	-1	20636.666	-2		
27.5	20635.874	2	20593.736	1	20614.432	4	20614.574	-6	20636.031	1	20593.877	-4
28.5	20635.178	1	20591.536	-2	20612.991	9	20613.140	-0	20635.339	-2	20591.685	-6
29.5	20634.432	0	20589.296	4	20611.487	0	20611.649	-1	20634.603	2	20589.453	4
30.5	20633.650	14	20586.995	0	20609.943	3	20610.110	0	20633.811	0	20587.159	1
31.5	20632.790	1	20584.653	6	20608.345	3	20608.517	-1	20632.965	-4	20584.815	-1
32.5	20631.893	3	20582.251	2	20606.699	5	20606.875	-1	20632.076	-1	20582.424	1
33.5	20630.941	0	20579.801	1	20604.994	-1	20605.182	-0	20631.137	4	20579.980	-1
34.5	20629.938	-2	20577.298	-2	20603.250	5	20603.440	2	20630.134	-5	20577.488	2
35.5	20628.889	-0	20574.752	2	20601.448	3	20601.643	-1	20629.094	0	20574.940	-3
36.5			20572.153	4	20599.600	6	20599.802	3			20572.349	1
37.5	20626.634	0	20569.502	3	20597.694	2	20597.900	-2	20626.848	-3	20569.707	4
38.5	20625.431	2	20566.792	-4	20595.739	1	20595.956	1	20625.650	-2	20567.012	5
39.5	20624.170	-4	20564.052	8	20593.736	1	20593.962	4	20624.404	1	20564.267	6
40.5	20622.864	-3	20561.243	2	20591.685	5	20591.913	3			20561.467	3
41.5	20621.510	-0	20558.392	5	20589.573	-2	20589.813	3	20621.754	3	20558.617	0
42.5	20620.098	-2	20555.478	-5	20587.419	1	20587.661	2	20620.352	3	20555.721	2
43.5			20552.527	-1	20585.212	1	20585.460	1	20618.899	4	20552.774	4
44.5	20617.131	1	20549.521	-2	20582.953	0	20583.208	1	20617.389	-1	20549.771	0
45.5	20615.568	1	20546.464	-2	20580.641	-2	20580.905	2	20615.828	-6	20546.719	-1
46.5	20613.944	-9			20578.284	1	20578.552	2	20614.222	-5	20543.624	3
47.5	20612.284	-5			20575.876	3	20576.144	-2	20612.572	4	20540.470	1
48.5	20610.577	4	20536.990	-4	20573.413	3	20573.691	2	20610.855	-4	20537.271	4
49.5	20608.808	4	20533.738	3	20570.894	-3	20571.187	4	20609.098	1	20534.016	1
50.5	20606.983	-3	20530.430	5	20568.337	4	20568.623	-3	20607.287	1	20530.708	-4
51.5	20605.106	-10	20527.064	-1	20565.717	-1	20566.016	-2	20605.427	5	20527.365	6
52.5			20523.653	-2	20563.056	4	20563.362	4			20523.955	1
53.5	20601.231	10	20520.195	3	20560.332	-2	20560.648	1	20601.532	-9	20520.505	6
54.5	20599.200	3	20516.685	6	20557.564	-3	20557.888	2			20516.988	-5
55.5	20597.119	-2	20513.107	-9	20554.746	-1	20555.071	-3	20597.462	7	20513.434	-2
56.5	20594.995	2	20509.507	4			20552.211	1	20595.329	-5	20509.837	7
57.5	20592.812	-3	20505.832	-5	20548.954	-0	20549.294	-1	20593.162	-0	20506.171	-0
58.5	20590.578	-5	20502.120	-2	20545.981	-1	20546.332	2	20590.939	-0	20502.462	-1
59.5	20588.296	-6	20498.351	-5	20542.963	5	20543.315	2	20588.667	3	20498.699	-5

TABLE 1—Continued

0 - 0												
J	Rec(J)	O-C	Pec(J)	O-C	Qef(J)	O-C	Qfe(J)	O-C	Rff(J)	O-C	Pff(J)	O-C
60.5	20585.963	-6	20494.543	4	20539.877	-6	20540.238	-7	20586.337	-1	20494.895	2
61.5	20583.588	5	20490.675	5	20536.757	1	20537.125	-1	20583.963	3	20491.037	5
62.5	20581.144	-2	20486.743	-9	20533.577	-2	20533.953	-3	20581.535	4	20487.120	-1
63.5	20578.652	-6	20482.788	7	20530.343	-7	20530.726	-8	20579.046	-4	20483.162	3
64.5	20576.122	4	20478.762	2	20527.064	-5	20527.460	-1	20576.522	5	20479.152	7
65.5			20474.684	-5	20523.736	-2	20524.135	-2	20573.931	-2	20475.079	-2
66.5			20470.565	-1	20520.355	-0	20520.758	-4	20571.296	-1	20470.961	-4
67.5	20568.178	-8	20466.394	1	20516.915	-6	20517.335	-1	20568.607	-3	20466.797	-3
68.5			20462.165	-4	20513.434	-1	20513.857	-1	20565.869	-1	20462.577	-6
69.5	20562.642	2	20457.890	-3	20509.900	2	20510.326	-3			20458.315	-0
70.5			20453.568	1	20506.305	-4	20506.749	1	20560.232	-4	20454.001	4
71.5	20556.884	-3	20449.189	-1	20502.670	0	20503.117	1	20557.341	0	20449.621	-6
72.5	20553.935	3	20444.763	3	20498.976	-2	20499.434	2			20445.208	2
73.5			20440.284	2	20495.235	-1	20495.694	-3			20440.735	-1
74.5	20547.872	5	20435.754	3	20491.437	-3	20491.905	-6			20436.203	-10
75.5			20431.168	-1	20487.592	-3	20488.074	0			20431.641	1
76.5	20541.587	-6	20426.534	-2			20484.179	-5			20427.006	-9
77.5	20538.377	-2	20421.847	-6	20479.748	-0	20480.240	-3				
78.5	20535.113	1			20475.747	-1	20476.253	1			20417.609	-4
79.5					20471.693	-2	20472.210	3			20412.827	-8
80.5					20467.590	-1	20468.113	1				
81.5					20463.436	1	20463.956	-8				
82.5					20459.233	6						
83.5					20454.974	6						
84.5					20450.661	4	20451.220	6				
85.5					20446.304	11	20446.857	-3				
86.5					20441.885	6	20442.459	5				
87.5					20437.408	-4	20438.000	3				
88.5							20433.492	4				
89.5							20428.935	9				
0 - 1												
J	Rec(J)	O-C	Pec(J)	O-C	Qef(J)	O-C	Qfe(J)	O-C	Rff(J)	O-C	Pff(J)	O-C
10.5					19609.742	-0	19609.793	-7				
11.5					19609.190	-10	19609.261	-2				
12.5												
13.5											19597.895	15
14.5					19607.283	-11	19607.367	-6			19596.440	-10
15.5					19606.552	-12	19606.650	-0			19594.971	-3
16.5	19618.972	8	19593.382	17	19605.789	1	19605.874	-5			19593.445	-5
17.5	19618.883	-10	19591.791	2	19604.956	-9	19605.064	3			19591.878	-2
18.5	19618.767	-8	19590.163	-4	19604.107	11	19604.201	4				
19.5	19618.618	8	19588.509	11	19603.175	-3	19603.296	10			19588.592	-8
20.5	19618.392	-6	19586.785	3	19602.216	2	19602.321	-6	19618.519	2	19586.881	-8
21.5			19585.014	-5			19601.322	1	19618.262	-2	19585.133	1
22.5	19617.829	-5	19583.218	9	19600.148	2	19600.271	2	19617.962	-1	19583.326	-2
23.5	19617.489	8	19581.333	-20	19599.038	-3	19599.172	2	19617.609	-7	19581.481	4
24.5	19617.084	4	19579.438	-12	19597.895	5	19598.025	1	19617.222	1	19579.576	-4
25.5	19616.627	-6			19596.695	4	19596.824	-7	19616.773	-6	19577.646	11
26.5	19616.148	10	19575.506	3	19595.453	8	19595.588	-4	19616.286	-5	19575.647	3
27.5	19615.606	9	19573.468	9	19594.153	1	19594.304	-0	19615.747	-7	19573.606	0
28.5	19615.006	-2	19571.361	-8	19592.811	-1	19592.971	0	19615.165	-6	19571.528	8
29.5	19614.367	-4	19569.228	-3	19591.422	-4	19591.588	-1	19614.544	3		
30.5					19589.994	2	19590.163	1				
31.5					19588.509	-2	19588.693	6				

TABLE 1—Continued

0 - 1												
J	Rec(J)	O-C	Pec(J)	O-C	Qef(J)	O-C	Qfe(J)	O-C	Rff(J)	O-C	Pff(J)	O-C
32.5	19612.188	8			19586.989	5	19587.160	-4			19562.715	2
33.5	19611.357	2	19560.205	-9	19585.415	6	19585.595	-1	19611.547	-1	19560.396	2
34.5	19610.495	13			19583.786	-1			19610.683	2	19558.036	8
35.5	19609.570	8	19555.431	7	19582.122	4	19582.319	2	19609.765	-3	19555.624	8
36.5			19552.963	5	19580.404	2	19580.593	-13	19608.806	0	19553.166	9
37.5	19607.586	5	19550.442	-4	19578.638	-1	19578.846	-4	19607.799	2	19550.654	4
38.5			19547.888	1	19576.829	1	19577.049	3	19606.742	-1	19548.101	4
39.5	19605.405	-5	19545.285	4	19574.970	-1	19575.191	-3	19605.645	5	19545.497	0
40.5			19542.635	7	19573.076	9	19573.294	-1	19604.488	-1	19542.845	-5
41.5	19603.043	-7	19539.930	3	19571.123	9	19571.361	11	19603.296	4	19540.159	2
42.5	19601.803	4			19569.112	-4	19569.363	6	19602.050	4		
43.5	19600.502	2	19534.384	-3			19567.321	3	19600.760	7	19534.630	1
44.5	19599.151	-2	19531.544	-3			19565.221	-10	19599.423	9	19531.795	0
45.5	19597.761	1	19528.660	1	19562.839	3	19563.098	2	19598.025	-1	19528.910	-3
46.5	19596.320	2	19525.729	4	19560.647	-2	19560.919	4	19596.596	4	19525.994	9
47.5	19594.823	-6	19522.739	-4	19558.414	1	19558.683	-4	19595.112	2	19523.003	-7
48.5			19519.715	0	19556.130	-1	19556.416	5	19593.576	-4	19519.997	9
49.5	19591.709	0			19553.801	-0	19554.089	1	19592.012	10		
50.5	19590.070	-8	19513.519	2	19551.435	10	19551.721	4	19590.378	1	19513.806	2
51.5	19588.415	17	19510.358	10	19549.002	1	19549.304	3	19588.705	1	19510.641	-0
52.5	19586.665	-6	19507.124	-8	19546.526	-3	19546.844	8	19586.989	5	19507.420	-11
53.5	19584.903	6					19544.329	6	19585.210	-6	19504.175	1
54.5	19583.067	-7	19500.558	0							19500.867	-4
55.5	19581.207	3	19497.191	-10							19497.524	3
56.5	19579.288	2	19493.789	-6	19536.175	6			19579.628	1	19494.123	1
57.5			19490.350	6	19533.464	4	19533.805	4	19577.665	-3	19490.667	-10
58.5	19575.312	5			19530.704	-1	19531.057	4	19575.650	-12	19487.184	-2
59.5					19527.890	-11	19528.261	5	19573.606	-2	19483.653	5
60.5					19525.041	-9	19525.406	-7				
61.5	19568.973	-7	19476.066	-0	19522.161	9	19522.522	0	19569.362	6	19476.434	5
62.5					19519.207	1	19519.577	-6			19472.757	8
63.5	19564.519	-2			19516.207	-6						
64.5					19513.179	8	19513.554	-9	19562.615	-5		
65.5	19559.863	-9			19510.077	-6	19510.481	-1	19560.269	-10		
66.5	19557.483	8			19506.955	8	19507.357	3	19557.886	-3		
67.5	19555.027	-3			19503.756	-7	19504.175	-2	19555.443	-9		
68.5	19552.533	-3			19500.532	1	19500.959	5	19552.963	-4		
69.5					19497.258	6	19497.684	2	19550.442	8		
70.5					19493.925	-0	19494.371	7				
71.5					19490.554	4						
72.5					19487.125	-3	19487.586	4				
73.5					19483.667	9	19484.121	0				
74.5					19480.142	2	19480.610	0				
75.5					19476.580	6	19477.060	7				
76.5					19472.965	5	19473.457	9				

Note: O-C are observed minus calculated line positions in units of 10^{-3} cm^{-1} .

OBSERVATION AND ANALYSIS

The spectral line positions were extracted from the observed spectra using a data reduction program called PC-DECOMP developed by J. Brault. The peak positions were determined by fitting a Voigt lineshape function to each spectral feature. The branches in different bands were sorted out using a color Loomis-Wood program running on a PC computer.

In addition to some TaN bands (21), most of the bands observed by Cheetham and Barrow (14) in the 17 000–28 000 cm^{-1} region are also present in our spectra. A close comparison of our spectra with the list of bands reported by Cheetham and Barrow (14) indicates that two new transitions of TaO with the 0–0 origins at 20 634.32758(40) and 22 188.88201(50) cm^{-1} are also present in our spectra. We have assigned these

TABLE 2
Observed Line Positions (in cm^{-1}) in the $K^2\Phi_{5/2}-X^2\Delta_{3/2}$ Transition of TaO

J	1 - 2						1 - 0					
	R(J)	O-C	Q(J)	O-C	P(J)	O-C	R(J)	O-C	Q(J)	O-C	P(J)	O-C
5.5									23086.082	-3		
6.5												
7.5									23085.377	-4		
8.5									23084.954	1	23078.552	4
9.5									23084.460	-15		
10.5									23083.935	-11	23076.025	-10
11.5	21057.047	5	21047.632	8			23092.777	-9	23083.360	-8	23074.701	-1
12.5	21057.267	8	21047.084	-4			23092.904	-6	23082.735	-3	23073.310	-10
13.5	21057.432	-1	21046.506	-2			23092.985	2	23082.053	-6	23071.889	2
14.5	21057.568	5	21045.882	-4	21034.966	4			23081.324	-4	23070.397	-8
15.5	21057.654	3	21045.219	-2			23092.985	7	23080.545	-4	23068.873	1
16.5	21057.693	-2	21044.510	-2	21032.084	2	23092.904	4	23079.717	-1		
17.5	21057.693	-3	21043.759	-2	21030.573	-6	23092.777	6	23078.834	-2	23065.646	-8
18.5	21057.654	-0	21042.965	-1	21029.021	-10	23092.593	1	23077.904	-1	23063.970	0
19.5	21057.568	-1	21042.128	-1	21027.443	2	23092.366	4	23076.921	-2	23062.235	-1
20.5	21057.432	-8	21041.250	1	21025.805	-3	23092.087	5	23075.889	-2	23060.448	-2
21.5	21057.267	-2	21040.327	2	21024.135	1	23091.759	8	23074.806	-1	23058.615	-0
22.5	21057.047	-7	21039.355	-4	21022.407	-7	23091.373	4	23073.674	-0	23056.728	-1
23.5	21056.803	7	21038.351	2	21020.647	-6	23090.939	2	23072.489	-1	23054.793	-1
24.5	21056.483	-11	21037.297	1	21018.845	-4	23090.451	-3	23071.257	2	23052.807	-1
25.5	21056.146	-4	21036.204	4	21017.003	2	23089.925	5	23069.970	-1	23050.770	-1
26.5	21055.767	5	21035.061	-0	21015.113	3	23089.334	-2	23068.633	-2		
27.5	21055.328	-4	21033.880	1	21013.176	-2	23088.701	0	23067.256	8	23046.549	3
28.5	21054.859	2	21032.655	1			23088.014	-0	23065.813	1	23044.357	-2
29.5	21054.349	10	21031.385	-0	21009.188	7	23087.283	5	23064.327	3	23042.124	4
30.5	21053.776	-1	21030.076	3	21007.118	-1	23086.496	6	23062.788	2	23039.828	-4
31.5	21053.174	1	21028.723	5	21005.014	-0	23085.654	2	23061.199	2	23037.494	1
32.5	21052.533	9	21027.322	3	21002.869	4	23084.762	-0	23059.559	1	23035.108	5
33.5	21051.834	1	21025.882	3	21000.674	0	23083.822	-0	23057.868	1	23032.654	-9
34.5	21051.107	10			20998.439	0	23082.835	4	23056.127	0	23030.171	-1
35.5	21050.314	-4	21022.866	1	20996.161	-1	23081.782	-7	23054.335	-0	23027.630	-1
36.5	21049.497	1	21021.291	-3	20993.833	-7	23080.696	1	23052.494	1		
37.5	21048.624	-6	21019.678	-1	20991.479	3	23079.556	5	23050.600	1	23022.397	-0
38.5	21047.719	-1			20989.067	-2	23078.343	-12	23048.657	2	23019.703	-2
39.5	21046.766	-0	21016.312	-7	20986.617	-2	23077.111	3	23046.662	2	23016.963	2
40.5			21014.574	0	20984.124	-1	23075.809	-2	23044.615	-0	23014.162	-4
41.5	21044.723	-5	21012.785	1	20981.589	0	23074.469	7	23042.520	2	23011.326	4
42.5	21043.650	7			20979.013	4	23073.061	-0	23040.372	1	23008.425	-1
43.5	21042.522	7	21009.070	-7	20976.384	-2	23071.610	-0	23038.171	-0	23005.473	-7
44.5	21041.342	-0	21007.160	3	20973.725	7	23070.107	-0	23035.925	3	23002.479	-4
45.5	21040.124	-3	21005.194	-1	20971.009	0	23068.551	-3	23033.622	0	22999.437	1
46.5	21038.866	0	21003.184	-4	20968.263	7	23066.951	3			22996.339	2
47.5			21001.140	2	20965.458	-1	23065.287	-4	23028.869	3	22993.189	1
48.5	21036.212	-1	20999.036	-7			23063.577	-6	23026.413	-0	22989.990	2
49.5			20996.907	2			23061.828	5	23023.908	1	22986.735	-3
50.5	21033.378	-6	20994.721	-3	20956.811	2	23060.011	-0	23021.350	-1	22983.443	7
51.5	21031.899	-5	20992.495	-4	20953.838	-1	23058.144	-4	23018.745	2		
52.5	21030.386	7	20990.233	3	20950.826	1	23056.231	-3	23016.086	2	22976.677	-3
53.5			20987.917	0	20947.767	-0	23054.266	-1	23013.375	1	22973.229	4
54.5	21027.188	-8	20985.563	3	20944.669	2	23052.251	2	23010.602	-11	22969.725	6
55.5	21025.541	2	20983.189	30			23050.176	-3	23007.802	2	22966.162	-1
56.5	21023.834	-2	20980.707	-7	20938.340	6	23048.056	-1	23004.933	-2	22962.542	-14
57.5	21022.088	-2	20978.230	5	20935.096	-6	23045.878	-6			22958.899	3
58.5	21020.296	-3	20975.695	3	20931.827	-0	23043.650	-9	22999.051	-0	22955.180	-6

TABLE 2—Continued

J	1 - 2						1 - 0					
	R(J)	O-C	Q(J)	O-C	P(J)	O-C	R(J)	O-C	Q(J)	O-C	P(J)	O-C
59.5	21018.456	-8	20973.114	-1			23041.383	2	22996.032	-1	22951.422	-3
60.5	21016.578	-6	20970.493	-0	20925.137	-8	23039.053	1	22992.962	0	22947.614	1
61.5			20967.837	9	20921.725	-13	23036.666	-4	22989.842	3	22943.745	-5
62.5			20965.131	13	20918.283	-5			22986.662	-3	22939.834	-0
63.5			20962.374	9			23031.754	3	22983.443	3	22935.863	-5
64.5			20959.570	4			23029.217	5	22980.159	-2	22931.843	-8
65.5							23026.617	-6	22976.828	-4	22927.783	1
66.5			20953.838	2					22973.447	-4	22923.660	-1
67.5			20950.901	-3			23021.283	-2	22970.023	6	22919.481	-9
68.5			20947.931	3			23018.539	2	22966.535	2	22915.274	8
69.5			20944.902	-6					22962.989	-7	22910.987	-4
70.5			20941.845	3							22906.664	-0
71.5			20938.748	16			23009.983	3	22955.765	1	22902.290	4
72.5							23007.014	-8				
73.5							23004.017	5			22893.364	-11
74.5							23000.961	12			22888.844	3
75.5							22997.837	5	22940.677	1	22884.267	11
76.5							22994.663	-1	22936.786	12	22879.619	1
77.5							22991.437	-5	22932.819	0		
78.5												
79.5									22924.757	6		
80.5									22920.648	11		
81.5												
82.5									22912.257	3		
83.5									22907.978	-4		
84.5									22903.655	-3		

J	0 - 1						0 - 0					
	R(J)	O-C	Q(J)	O-C	P(J)	O-C	R(J)	O-C	Q(J)	O-C	P(J)	O-C
6.5	21171.777	-14							22187.747	-0		
7.5	21172.216	-11					22193.838	2	22187.402	3		
8.5	21172.608	-12	21165.420	-5			22194.189	-8	22186.994	-9		
9.5	21172.963	-6	21165.019	0			22194.508	-4	22186.547	-15	22179.348	-18
10.5	21173.278	1	21164.562	-7			22194.775	-6	22186.067	-5	22178.112	-9
11.5	21173.541	-1	21164.067	-9	21155.355	-13	22194.998	-4	22185.520	-17	22176.821	-8
12.5	21173.762	-1	21163.534	-6	21154.075	-0	22195.170	-7	22184.950	-5	22175.480	-10
13.5	21173.945	4	21162.961	-1					22184.327	0	22174.098	-7
14.5	21174.081	4	21162.344	3	21151.359	-3			22183.654	2	22172.663	-9
15.5			21161.674	-3	21149.939	-2			22182.928	-2	22171.193	-1
16.5			21160.970	0	21148.469	-8			22182.166	4	22169.668	-2
17.5			21160.218	-1					22181.348	1	22168.099	1
18.5	21174.193	5	21159.424	-2	21145.418	-3	22195.247	-0	22180.485	-0	22166.478	-2
19.5	21174.107	-0	21158.590	-0			22195.098	4	22179.574	-3	22164.813	-3
20.5	21173.981	-3	21157.719	8	21142.193	-1	22194.898	2	22178.626	3	22163.112	7
21.5	21173.819	0	21156.794	4	21140.525	9	22194.656	5	22177.624	3		
22.5	21173.608	-1	21155.828	3	21138.794	-2	22194.356	-2	22176.575	2	22159.543	-1
23.5	21173.361	4	21154.819	2	21137.035	2	22194.021	3	22175.480	2	22157.695	2
24.5	21173.065	3	21153.768	2			22193.633	2	22174.337	1	22155.791	-5
25.5	21172.724	1	21152.678	6	21133.377	0	22193.191	-7	22173.155	7	22153.860	8
26.5	21172.344	3	21151.540	5	21131.490	5	22192.718	-1	22171.915	2	22151.864	2
27.5	21171.921	5	21150.354	-1	21129.546	-3	22192.192	1	22170.634	4	22149.828	4
28.5	21171.450	2	21149.133	1	21127.562	-10	22191.615	-2	22169.303	1		
29.5	21170.944	9	21147.866	1			22190.998	2	22167.927	1	22145.612	1

TABLE 2—Continued

J	0 - 1						0 - 0					
	R(J)	O-C	Q(J)	O-C	P(J)	O-C	R(J)	O-C	Q(J)	O-C	P(J)	O-C
30.5	21170.381	1	21146.555	-1	21123.489	2	22190.330	2	22166.499	-4	22143.435	1
31.5	21169.786	5	21145.196	-8	21121.381	1	22189.615	3	22165.039	4	22141.212	1
32.5	21169.147	7	21143.816	9	21119.225	-5	22188.850	0	22163.520	2	22138.944	3
33.5	21168.456	2	21142.369	-0	21117.046	9	22188.043	2			22136.631	7
34.5			21140.886	-1	21114.803	1	22187.162	-22	22160.347	2	22134.262	2
35.5	21166.960	6	21139.362	0	21112.521	-1	22186.284	4	22158.688	-1	22131.856	6
36.5	21166.130	-7	21137.794	1	21110.194	-7	22185.333	4	22156.981	-3	22129.395	2
37.5	21165.277	-1	21136.177	-4	21107.839	2	22184.327	-4	22155.232	-2	22126.889	1
38.5	21164.373	-2	21134.527	2			22183.284	-1	22153.436	1	22124.336	-2
39.5	21163.425	-4	21132.826	-0	21102.974	-3			22151.593	3	22121.741	-0
40.5	21162.445	6	21131.078	-7	21100.484	0	22181.058	6	22149.699	1	22119.095	-1
41.5	21161.410	6	21129.299	-0	21097.942	-3	22179.862	-2	22147.754	-5	22116.409	3
42.5			21127.469	-2	21095.363	-2	22178.626	-3	22145.773	1	22113.669	1
43.5	21159.200	-6	21125.591	-7	21092.743	1	22177.348	1	22143.738	-1	22110.892	9
44.5	21158.041	0	21123.682	-0	21090.075	0			22141.660	1	22108.043	-8
45.5			21121.714	-9	21087.368	3	22174.634	-5	22139.529	-1	22105.179	7
46.5	21155.571	-8	21119.720	0	21084.609	-2		0	22137.356	1	22102.245	-2
47.5	21154.281	-1	21117.677	3	21081.812	-4	22171.747	6	22135.133	1	22099.275	1
48.5	21152.940	-2	21115.583	-1	21078.976	1	22170.229	8	22132.864	2	22096.253	-1
49.5	21151.552	-5	21113.450	0	21076.091	-1	22168.654	1	22130.546	1	22093.186	-1
50.5	21150.130	2	21111.268	-5	21073.160	-6	22167.034	-2	22128.183	2	22090.078	4
51.5	21148.651	-4	21109.050	-1	21070.187	-8	22165.372	-1	22125.767	-2	22086.924	11
52.5			21106.790	4	21067.179	-3	22163.660	-1	22123.310	1	22083.703	-2
53.5	21145.582	4	21104.477	-1	21064.122	-4			22120.802	-0	22080.452	2
54.5	21143.975	2	21102.116	-9			22160.104	8	22118.251	4	22077.145	-3
55.5			21099.737	8	21057.900	18	22158.243	3	22115.650	5	22073.798	0
56.5	21140.622	-8	21097.287	-2			22156.337	0	22112.999	3	22070.395	-6
57.5	21138.895	3	21094.803	-2	21051.471	7	22154.383	-3	22110.302	4	22066.958	1
58.5	21137.106	-4	21092.275	-1			22152.394	8	22107.551	-2	22063.468	2
59.5			21089.712	8	21044.872	2	22150.338	-2	22104.760	-1		
60.5	21133.412	1	21087.088	0	21041.517	8	22148.242	-1	22101.918	-2		
61.5	21131.494	-1	21084.425	-2					22099.031	-0	22052.714	6
62.5			21081.721	-2	21034.651	-4			22096.097	2		
63.5			21078.976	2	21031.154	-7	22141.660	-8	22093.110	-1	22045.305	7
64.5	21125.472	-9	21076.178	-4	21027.623	-1	22139.384	5	22090.078	-1	22041.524	2
65.5	21123.387	1	21073.345	1	21024.034	-10	22137.057	16	22087.002	3	22037.697	-1
66.5	21121.242	-6	21070.465	2			22134.654	-2	22083.867	-3	22033.829	2
67.5	21119.055	-9	21067.535	-1			22132.222	1	22080.694	0	22029.911	3
68.5	21116.837	1	21064.564	-2			22129.736	-3			22025.942	0
69.5	21114.566	5	21061.553	1			22127.207	-1	22074.193	-4		
70.5	21112.234	-9	21058.491	-1			22124.630	3	22070.885	9	22017.866	-0
71.5	21109.883	3	21055.394	6			22121.994	-4	22067.508	1	22013.751	-4
72.5	21107.474	3	21052.247	8					22064.085	-5	22009.602	4
73.5			21049.038	-9			22116.595	1	22060.624	0	22005.391	-1
74.5									22057.117	7	22001.139	-0
75.5			21042.522	-4					22053.546	-1	21996.828	-9
76.5			21039.207	8			22108.123	2	22049.935	-0	21992.483	-5
77.5			21035.827	0							21988.100	10
78.5			21032.428	19							21983.643	-2
79.5			21028.933	-14					22038.818	8	21979.139	-12
80.5			21025.438	-1					22035.005	1	21974.610	2
81.5									22031.151	1	21970.026	8
82.5									22027.249	3	21965.382	3
83.5									22023.298	5	21960.694	1
84.5									22019.296	4	21955.951	-6
85.5									22015.232	-9		

TABLE 2—Continued

2 - 1													
J	R(J)	O-C	Q(J)	O-C	P(J)	O-C	J	R(J)	O-C	Q(J)	O-C	P(J)	O-C
7.5	22960.773	-1	22954.400	-1			41.5	22943.240	-10	22911.469	2		
8.5	22961.089	-7	22953.962	-11	22947.602	2	42.5	22941.844	2	22909.311	-4		
9.5	22961.363	-3	22953.495	1	22946.377	5	43.5	22940.395	12	22907.109	-4	22874.586	-1
10.5			22952.961	-4	22945.087	-6	44.5	22938.861	-11	22904.861	2	22871.593	3
11.5			22952.375	-10	22943.761	-3	45.5	22937.311	1	22902.552	-3	22868.544	2
12.5					22942.388	4	46.5	22935.698	1	22900.203	4	22865.436	-7
13.5	22961.942	-1	22951.071	-3	22940.942	-12	47.5	22934.035	3			22862.300	7
14.5	22961.954	-7	22950.344	1	22939.481	7	48.5	22932.313	-2	22895.334	1	22859.097	3
15.5	22961.942	14	22949.559	-2	22937.934	-10	49.5	22930.546	-1	22892.818	-6	22855.837	-5
16.5	22961.854	8	22948.728	-2	22936.372	10	50.5	22928.726	-1	22890.262	-1	22852.542	3
17.5	22961.721	10	22947.849	2	22934.727	-4	51.5			22887.649	-1	22849.194	8
18.5	22961.536	9	22946.914	0	22933.045	-3	52.5			22884.988	1	22845.781	-0
19.5	22961.294	3	22945.930	1	22931.308	-8	53.5	22922.961	4	22882.278	7		
20.5	22960.998	-8	22944.896	1	22929.530	-4	54.5	22920.924	-7	22879.498	-7	22838.825	6
21.5	22960.680	11	22943.809	-1	22927.700	-1	55.5	22918.851	0	22876.687	0		
22.5	22960.282	0	22942.674	-1	22925.816	-1	56.5	22916.717	-4	22873.812	-5		
23.5	22959.849	5	22941.494	4	22923.870	-13	57.5	22914.537	-2	22870.897	1	22827.989	-3
24.5	22959.363	8	22940.254	1	22921.905	7	58.5	22912.305	1	22867.921	-2	22824.281	1
25.5	22958.818	3	22938.962	-3	22919.870	7	59.5	22910.019	2	22864.904	6	22820.520	3
26.5	22958.224	-1	22937.627	-1	22917.780	2	60.5			22861.816	-6		
27.5	22957.578	-5	22936.241	2			61.5	22905.292	5	22858.701	8		
28.5	22956.896	5	22934.802	2	22913.466	10	62.5	22902.852	8	22855.506	-7		
29.5	22956.149	1	22933.311	1	22911.221	3	63.5	22900.353	5	22852.273	-9		
30.5			22931.769	-1	22908.931	0	64.5			22848.999	1		
31.5	22954.514	5	22930.181	3	22906.586	-7	65.5			22845.664	1		
32.5	22953.611	-2	22928.539	3	22904.207	3	66.5	22892.546	-1	22842.273	-3		
33.5	22952.661	-5	22926.845	3	22901.769	4	67.5			22838.825	-11		
34.5							68.5	22887.082	-2				
35.5	22950.610	-9	22923.296	-8	22896.738	4	69.5	22884.267	-7	22831.805	6		
36.5	22949.519	0	22921.461	2	22894.152	8	70.5			22828.203	-1		
37.5	22948.362	-6	22919.565	3	22891.498	-4	71.5			22824.555	-1		
38.5	22947.164	-1	22917.612	-3	22888.811	2	72.5			22820.852	-3		
39.5	22945.918	7	22915.611	-5	22886.068	2	73.5			22817.107	5		
40.5			22913.566	-1	22883.265	-8	74.5			22813.300	4		

Note: O-C are observed minus calculated line positions in units of 10^{-3} cm^{-1} .

transitions as $H^2\Pi_{1/2}-X^2\Delta_{3/2}$ and $K^2\Phi_{5/2}-X^2\Delta_{3/2}$ after a rotational analysis and comparison with the matrix absorption (18) and MCD matrix isolation results (19).

The 0-0 and 0-1 bands of the $H^2\Pi_{1/2}-X^2\Delta_{3/2}$ transition are located near 20 640 and 19 619 cm^{-1} , respectively. The 0-0 band of this transition was observed at 20 804 cm^{-1} in a neon matrix and at 20 919 cm^{-1} in an Ar matrix (18) and $\Omega = 1/2$ was assigned to the excited state on the basis of the MCD matrix isolation experiment. Each of these bands consist of R, P, and Q branches, all doubled due to presence of Ω -doubling in the $H^2\Pi_{1/2}$ state. A part of the 0-0 band near the R head is presented in Fig. 1 where some low-J, -R, and -Q lines have been marked. Some high-J lines of this band are presented in Fig. 2 where the Ω -doubling observed in R, P, and Q branches is clearly evident. Apart from the 0-0 and 0-1 bands no other bands belonging to this transition could be identified in our

spectra because of their weak intensity. We have obtained a rotational analysis of the 0-0 and 0-1 bands and find them free of local perturbations.

To higher wavenumbers, another new transition with a 0-0 R head near 22 195 cm^{-1} has been identified. This band also consists of R, P, and Q branches, but in this case no Ω -doubling has been observed even for the highest J lines observed. The excited state of this transition, therefore, has been identified as $^2\Phi_{5/2}$. This transition corresponds to a state labeled as K by Weltner and McLeod (18) and was observed at 22 333 cm^{-1} in a neon matrix and at 22 201 cm^{-1} in a Ar matrix. The Ω -assignment of $\Omega = 5/2$ (with $^2\Phi$ symmetry) by Brittain *et al.* (19) is consistent with our present observations. We have, therefore, labeled this transition as the $K^2\Phi_{5/2}-X^2\Delta_{3/2}$ electronic transition. A part of the 1-0 band of this transition near the R head is presented in Fig. 3 with some low-J, -R, and -Q

TABLE 3
Molecular Constants (in cm^{-1}) for the $X^2\Delta_{3/2}$, $H^2\Pi_{1/2}$, and $K^2\Phi_{5/2}$ States of TaO

Const. ^a	$X^2\Delta_{3/2}$			$H^2\Pi_{1/2}$	$K^2\Phi_{5/2}$		
	v=0	v=1	v=2	v=0	v=0	v=1	v=2
T_v	0.0	1021.72746(63)	2036.27637(96)	20634.32758(40)	22188.88201(50)	23086.98486(55)	23977.73570(88)
B_v	0.4019690(31)	0.4001167(32)	0.3982607(33)	0.3766867(31)	0.3787043(32)	0.3768102(31)	0.3749169(32)
$10^7 \times D_v$	2.4712(42)	2.4736(44)	2.4791(47)	2.6118(43)	2.7602(44)	2.7702(43)	2.7802(45)
$10^3 \times p_v$	--	--	--	-5.292(14)	--	--	--
$10^7 \times p_{Dv}$	--	--	--	-1.743(33)	--	--	--

^aNumbers in parentheses are one standard deviation in the last two digits.

lines marked. We have obtained a rotational analysis of the 0–1, 1–2, 0–0, 1–0, and 2–1 bands of this transition, again without finding any perturbations.

Although the first lines in the different bands were not identified because of overlapping from lines returning from the head, a rotational assignment could be accomplished by comparing combination differences for the common vibrational levels. The lines from both the transitions were initially fitted separately using a simple empirical energy expression given as follows:

$$F_v(J) = T_v + B_v J(J+1) - D_v [J(J+1)]^2 \pm 1/2 [p_v(J+1/2) + p_{Dv}(J+1/2)^3]. \quad [1]$$

In the final fit the lines from both $H^2\Pi_{1/2}-X^2\Delta_{3/2}$ and $K^2\Phi_{5/2}-X^2\Delta_{3/2}$ transitions were combined and fitted simultaneously in order to obtain a single set of molecular constants for the $X^2\Delta_{3/2}$, $H^2\Pi_{1/2}$, and $K^2\Phi_{5/2}$ states. The lines in different bands were weighted depending on the signal-to-noise ratio and the extent of blending. The e/f parity assignment in different transitions was chosen arbitrarily to provide negative Ω -doubling constants in the excited $H^2\Pi_{1/2}$ state, since there is no observable Ω -doubling present in the ground $X^2\Delta_{3/2}$ state. The observed line positions for the $H^2\Pi_{1/2}-X^2\Delta_{3/2}$ and $K^2\Phi_{5/2}-X^2\Delta_{3/2}$ transitions are provided in Tables 1 and 2 respectively, and the molecular constants for the $X^2\Delta_{3/2}$, $H^2\Pi_{1/2}$, and $K^2\Phi_{5/2}$ states are provided in Table 3.

DISCUSSION

The transitions observed by Cheetham and Barrow (14) either involve the $X^2\Delta_{3/2}$ or the $X^2\Delta_{5/2}$ spin components of the ground state. The relative position of various electronic states was established by observing the $N^2\Delta_{3/2}-X^2\Delta_{5/2}$ and $N^2\Delta_{3/2}-X^2\Delta_{3/2}$ transitions originating from the same excited

state. This observation established that the $X^2\Delta_{5/2}$ spin component lies 3505 cm^{-1} above the lowest $X^2\Delta_{3/2}$ spin component suggesting a $^2\Delta_r$ ground state. However a low-lying $^4\Sigma^-$ state is also expected to be present based on the isovalent VO (9–11), NbO (12, 13), CrN (23), MoN (24–26), and WN (27) molecules. In fact all of these molecules have $^4\Sigma^-$ ground states. There are no high level ab initio calculations available for the low-lying states of TaO. The electronic structure of TaO resembles that of WCH molecule which was recently investigated by laser excitation spectroscopy (28). The ground state of WCH has been identified as $^2\Delta_{3/2}$ arising from the $\sigma^2\delta$ configuration. The $^4\Sigma^-_{1/2}$ state of WCH was located at 813 cm^{-1} above the ground state and was suggested to arise from the $\sigma\delta^2$ configuration. A similar pattern probably exists for TaO with the $^4\Sigma^-$ state arising from the $\sigma\delta^2$ configuration lying above the $^2\Delta_r$ ground state which arises from the $\sigma^2\delta$ configuration. It is surprising to note that no transitions of TaO involving quartet states have been identified.

The $^2\Delta_r$ state of VO, analogous to the $X^2\Delta_r$ state of TaO, is well characterized experimentally. Although the $^2\Delta-^4\Sigma^-$

TABLE 4
Equilibrium Constants (in cm^{-1}) for the $X^2\Delta_{3/2}$ and $K^2\Phi_{5/2}$ States of TaO

Constant ^a	$X^2\Delta_{3/2}$	$K^2\Phi_{5/2}$
ω_e	1028.9060(15)	905.4549(15)
$\omega_e x_e$	3.58928(66)	3.67601(64)
B_e	0.40289737(139)	0.37965102(36)
α_e	0.00185445(83)	0.00189370(21)
$r_e(\text{\AA})$	1.6873430(29)	1.7382343(8)

^a Numbers in parentheses are one standard deviation in the last two digits.

separation is not known precisely, a separation of $\sim 10\,000\text{ cm}^{-1}$ has been suggested by Merer *et al.* (10). The spectroscopic properties of other low-lying electronic states are provided by Bauschlicher *et al.* (29). For NbO, a $^2\Delta-^4\Sigma^-$ separation of 0.4 eV has been suggested by Dyke *et al.* (20) from their photoelectron study combined with ab initio calculations. The lowest $^2\Delta$ state and a number of other doublet excited states of NbO have recently been observed by Launila *et al.* (30). For TaO, Dyke *et al.* (20) predict that the $^4\Sigma^-$ state lies above the $^2\Delta$ state by 0.02 eV which is obviously very small and is unreliable based on the nature of their calculations.

The molecular constants of Table 3 have been used to evaluate the equilibrium constants for the $X^2\Delta_{3/2}$ and $K^2\Phi_{5/2}$ states which are provided in Table 4. The present ground state constants are in excellent agreement with the values of Cheetham and Barrow (14) but are expected to be more accurate by at least an order of magnitude. All of the known transitions of TaO terminate either in the $X^2\Delta_{3/2}$ or $X^2\Delta_{5/2}$ spin components of the ground state, suggesting that all known excited states are the spin components of various doublet electronic states. Because of the large spin-orbit splitting of 3505 cm^{-1} , the $X^2\Delta_r$ state is best described as intermediate between Hund's case (a) and case (c). Since transitions involving the $^4\Sigma_{1/2}^-$ spin component have characteristic $\pm 4B$ branches in addition to $\pm B$ and $\pm 2B$ branches, it is almost certain that no transitions involving the $^4\Sigma^-$ lower state have been observed so far.

The equilibrium constants for the $X^2\Delta_{3/2}$ and $K^2\Phi_{5/2}$ states have been used to evaluate the effective equilibrium bond lengths for these states (Table 4). The ground state bond length of $1.6873430(29)\text{ \AA}$ for TaO can be compared with the bond lengths of 1.59204_8 \AA for VO (11) and 1.68519_7 \AA for NbO (13) calculated from their respective B values, although they arise from different configurations than in TaO. A value of 1.732 \AA for TaO was calculated by Dyke *et al.* (20) from their Hartree-Fock-Slater calculations.

Unlike for the VO and NbO molecules, no hyperfine broadening was noticed in any of the TaO bands, although tantalum has a spin of $7/2$ and nuclear magnetic moment of $+2.37$ nuclear magnetons. This may be due to a cancellation of hyperfine effects in the ground and excited states. Of the many transitions observed by Cheetham and Barrow (14), a little hyperfine broadening was observed only in the $D-X^2\Delta_{3/2}$ system, which was not rotationally analyzed. Several of the excited states labeled by F , G , I , J , and O in the matrix spectra remain still to be observed in gas phase. We do not find any unassigned bands in our spectra which could be attributed to these states. Probably these transitions are relatively weak in intensity. After we completed our analysis, we learned that the $H^2\Pi_{1/2}-X^2\Delta_{3/2}$ and $K^2\Phi_{5/2}-X^2\Delta_{3/2}$ band systems were also observed in Stockholm (31).

CONCLUSION

The high-resolution emission spectrum of TaO has been recorded in the $10\,000-30\,000\text{ cm}^{-1}$ region using a Fourier transform spectrometer. In addition to previously reported transitions (14), two new electronic transitions with the 0-0 band origins at $20\,634.32758(40)$ and $22\,188.88201(50)\text{ cm}^{-1}$ have been assigned as the $H^2\Pi_{1/2}-X^2\Delta_{3/2}$ and $K^2\Phi_{5/2}-X^2\Delta_{3/2}$ transitions. The excited states of these transitions have previously been observed in matrix absorption experiments (18) and their Ω -assignments are consistent with the results of MCD matrix isolation experiments (19). A rotational analysis of a number of bands of these transitions has been carried out and molecular constants for the $H^2\Pi_{1/2}$ and $K^2\Phi_{5/2}$ states have been obtained for the first time. The $X^2\Delta_{3/2}$ ground state spin component of TaO has a bond length of $r_e = 1.6873430(29)\text{ \AA}$, compared with $r_0 = 1.59204_8\text{ \AA}$ for VO (11) and $r_0 = 1.68519_7\text{ \AA}$ for NbO (13).

ACKNOWLEDGMENTS

We thank J. Wagner and C. Plymate of the National Solar Observatory for assistance in obtaining the spectra. The National Solar Observatory is operated by the Association of Universities for Research in Astronomy, Inc., under contract with the National Science Foundation. The research described here was supported by funding from the NASA laboratory astrophysics program. Some support was also provided by the Natural Sciences and Engineering Research Council of Canada.

REFERENCES

1. H. Spinard and R. F. Wing, *Annu. Rev. Astr. Astrophys.* **7**, 269-302 (1969).
2. A. J. Merer, *Annu. Rev. Phys. Chem.* **40**, 407-438 (1989).
3. P. W. Merrill, A. J. Deutsch, and P. C. Keenan, *Astrophys. J.* **136**, 21-34 (1962).
4. H. Machara and Y. Y. Yamashita, *Publ. Astron. Soc. Japan* **28**, 135-140 (1976).
5. D. L. Lambert and R. E. S. Clegg, *Mon. Not. R. Astron. Soc.* **191**, 367-389 (1978).
6. S. Wyckoff and R. E. S. Clegg, *Mon. Not. R. Astron. Soc.* **184**, 127-143 (1978).
7. N. M. White and R. F. Wing, *Astrophys. J.* **222**, 209-219 (1978).
8. A. J. Sauval, *Astron. Astrophys.* **62**, 295-298 (1978).
9. A. J. Merer, A. S.-C. Cheung, and A. W. Taylor, *J. Mol. Spectrosc.* **108**, 343-351 (1984).
10. A. J. Merer, G. Huang, A. S.-C. Cheung, and A. W. Taylor, *J. Mol. Spectrosc.* **125**, 465-503 (1987).
11. A. G. Adam, M. Barnes, B. Bero, R. D. Bower, and A. J. Merer, *J. Mol. Spectrosc.* **170**, 94-130 (1987).
12. J. L. Féménias, G. Cheval, A. J. Merer, and U. Sassenberg, *J. Mol. Spectrosc.* **124**, 348-368 (1987).
13. A. G. Adam, Y. Azuma, J. A. Berry, A. J. Merer, U. Sassenberg, J. O. Schröder, G. Cheval, and J. L. Féménias, *J. Chem. Phys.* **100**, 6240-6262 (1994).
14. C. J. Cheetham and R. F. Barrow, *Trans. Faraday Soc.* **63**, 1835-1845 (1967).
15. C. C. Kiess and E. Z. Stowell, *Bur. Standards J. Res.* **12**, 459-469 (1934).
16. D. Premswarup, *Nature*, **175**, 1003-1003 (1955).
17. D. Premswarup and R. F. Barrow, *Nature*, **180**, 602-603 (1957).

18. W. Weltner, Jr. and D. McLeod, Jr., *J. Chem. Phys.* **42**, 882–891 (1965).
19. R. Brittain, D. Powell, M. Kreglewski, and M. Vala, *Chem. Phys.* **54**, 71–78 (1980).
20. J. M. Dyke, A. M. Ellis, M. Fehr, A. Morris, A. J. Paul, and J. C. H. Stevens, *J. Chem. Soc. Faraday Trans. II*, **83**, 1555–1565 (1987).
21. T. M. Dunn, private communication.
22. B. A. Palmer and R. Engleman, “Atlas of the Thorium Spectrum,” Los Alamos National Laboratory, Los Alamos, NM, 1983.
23. W. J. Balfour, C. X. W. Qian, and C. Zhou, *J. Chem. Phys.* **106**, 4383–4388 (1997).
24. R. C. Carlson, J. K. Bates, and T. M. Dunn, *J. Mol. Spectrosc.* **110**, 215–241 (1985).
25. K. J. Jung, D. A. Fletcher, and T. C. Steimle, *J. Mol. Spectrosc.* **165**, 448–456 (1994).
26. N. S.-K. Sze and A. S.-C. Cheung, *J. Mol. Spectrosc.* **173**, 194–204 (1995).
27. R. S. Ram and P. F. Bernath, *J. Opt. Soc. Am.* **11**, 225–230 (1994).
28. M. Barnes, D. A. Gillett, A. J. Merer, and G. F. Metha, *J. Chem. Phys.* **105**, 6168–6182 (1996).
29. C. W. Bauschlicher and S. R. Langhoff, *J. Chem. Phys.* **85**, 5936–5942 (1986).
30. O. Launila, B. Schimmelpfennig, H. Fagerli, O. Gropen, A. G. Taklif, and U. Wahlgren, *J. Mol. Spectrosc.* **186**, 131–143 (1997).
31. A. Al-Khalili and O. Launila, private communication.